Sensors and Control Concept of a Biped Robot

Klaus Löffler, Michael Gienger, Friedrich Pfeiffer, *Fellow, IEEE*, and Heinz Ulbrich

***Abstract*—The biped robot "Johnnie" is designed to achieve a dynamically stable gait pattern, allowing for high walking velocities. Very accurate and fast sensors were developed for the machine. In particular, the design of the three-dimensional-orientation sensor and the six-axes force–torque sensor are presented. The control scheme is based on the information from these sensors to deal with unstructured terrain and disturbances. Two different implementations are investigated: a computed torque approach and a trajectory control with adaptive trajectories. Walking speeds of 2.4 km/h have been achieved in experiments.**

***Index Terms*—Cascade control, legged locomotion, microcontrollers, mobile robot dynamics, motion control, motion planning, multisensor systems, torque control.**

I. Introduction

In the past several years, the development of sophisticated biped walking robots has increased rapidly. Key developments have been achieved, as reported in [5] and [6], where powerful biped walking robots were developed. The goals of this research project are the realization of a biped robot that is able to walk dynamically stable on even and uneven ground and around curves. It is also planned to realize a fast dynamically stable walking motion as well as slow "jogging" with flight phases. Up to now a walking speed of 2.4 km/h has been achieved in experiments and trajectories for higher velocities are currently being implemented. Fig. 1 shows the assembled robot "Johnnie" [3], [7], [8], [11] of the Institute for Applied Mechanics, Technical University of Munich (TUM), Garching, Germany. The development is based on comprehensive experience, that has been obtained in the development of two multilegged walking machines [10], [13], [17] and general research in the area of robotic systems [12], [15]. The vision system has been developed at the Institute of Automatic Control Engineering of the TUM [14]. The robot is equipped with 17 joints. Each leg is driven with six joints, three in the hip, one in the knee, and two (pitch and roll) in the ankle. The upper body has one degree of freedom (DOF) about the vertical axis of the pelvis. To compensate for the overall moment of momentum,

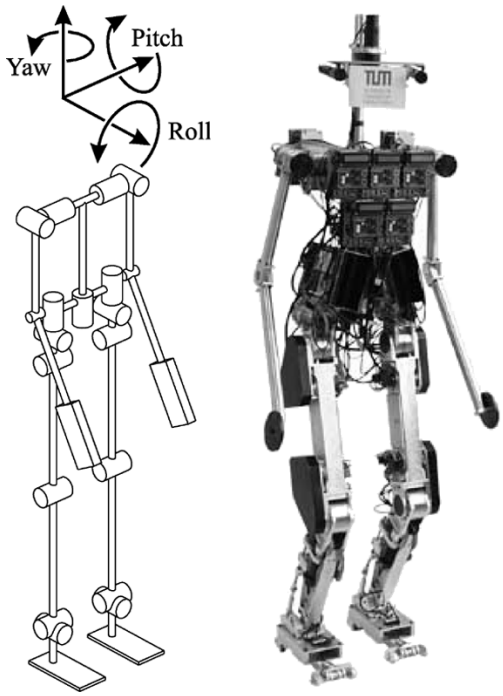

Fig. 1. "Johnnie."

each shoulder incorporates 2 DOF. The geometry of the machine corresponds to that of a male human with a body height of 1.8 m.[1] The total weight is about 40 kg. The biped is autonomous to a far extent, only the energy and a part of the computational power is supplied by cables.

II. Sensor System

A. Joint Sensors

Each joint is equipped with an incremental encoder (HP 5550) that is attached to the motor shaft. The encoders have two channels with 500 lines and one channel with a reference line. Such an accuracy of 1/2000 of a revolution is obtained using standard microcontroller hardware. The reference position for the measurement is obtained by light barriers.

B. Force Sensors

The biped robot is equipped with two six-axes force/torque sensors that are integrated in the foot. The forces and torques acting on the foot during a jogging motion have been determined with a detailed multibody simulation program. Based on these data and multiple iterations of finite-element analysis, an optimal design was developed (Fig. 2). The sensor consists of a

Manuscript received November 4, 2002; revised January 22, 2004. Abstract published on the Internet July 15, 2004. This work was supported by the "Deutsche Forschungsgemeinschaft" within the priority program "Autonomous Walking." This paper was presented at the IEEE 7th International Workshop on Advanced Motion Control, Maribor, Slovenia, July 3–5, 2002.

K. Löffler was with the Institute for Applied Mechanics, Technical University of Munich, 85747 Garching, Germany. He is now with BMW AG, 80788 Munich, Germany (e-mail: Klaus.Loeffler@bmw.de).

M. Gienger was with the Institute for Applied Mechanics, Technical University of Munich, 85747 Garching, Germany. He is now with the Honda Research Institute Europe GmbH, D-63073 Offenbach/Main, Germany.

F. Pfeiffer and H. Ulbrich are with the Institute for Applied Mechanics, Technical University of Munich, 85747 Garching, Germany.

Digital Object Identifier 10.1109/TIE.2004.834948

[1] U. Hahn, Calculation of anthropometric data for human body segments, implemented in software program "Calcman3d," 1994.

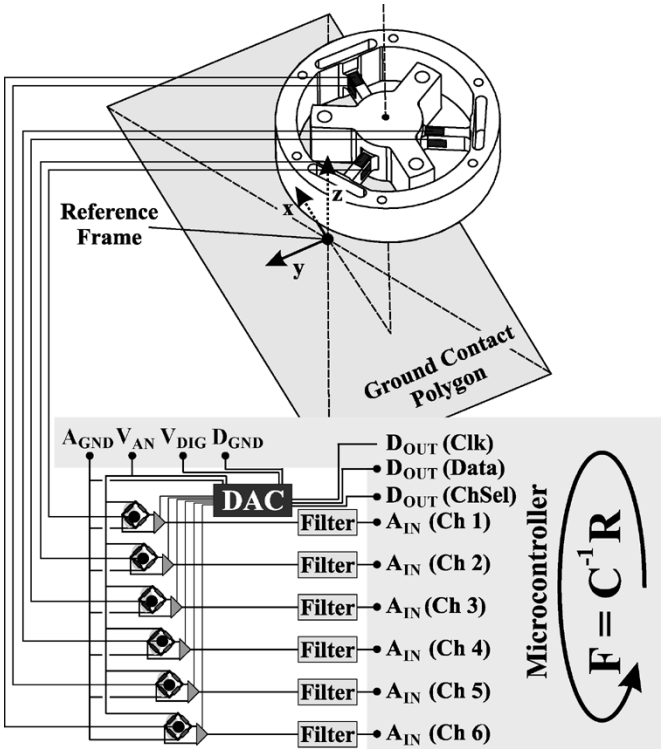

Fig. 2. Force sensor design.

TABLE I
ORIENTATION SENSOR

Gyros	Silicon Sensing Systems	CRS 04
	Bandwidth	85 Hz
	Range	+/-150 deg/s
Accelerometer	Crossbow	CXL02TG3
	Range	+/-2 g

single aluminum part. Three deformation beams holding strain gauges are within the load path. Two opposing strain gauges operate as a half bridge, compensating for temperature dependency. Thin membranes mechanically decouple the individual beam deflections to a great extent and so reduce cross talk. Special emphasis has been devoted to the strain-gauge application. The strain gauges are selected to match the elastic properties of the sensor material. An exact application in combination with an appropriate temperature treatment finally lead to a high zero point stability of the signal.

C. Attitude Sensor

The orientation of the robot is determined by a combination of gyroscopes and accelerometers. The technical data of the sensors used are depicted in Table I. The acceleration sensors provide correct signals in the static case, but the information is disturbed by translational accelerations. On the other hand, a pure integration of the gyroscopic angular velocity data leads to an unbounded error due to noise and disturbances. To overcome these problems, a variety of sensor fusion methods have been proposed [2], [9]. The scheme that is employed here is based on complementary filtering the gyro- and accelerometer signals. The basic idea is to weight the sensor data in frequency ranges in which the respective sensor can be considered as ideal. Fig. 3

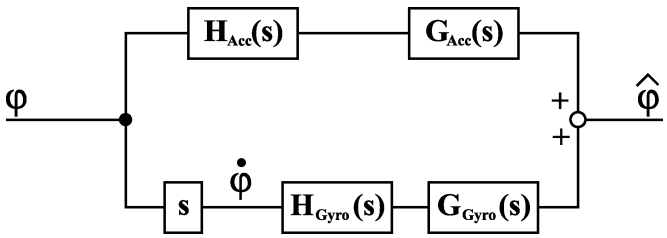

Fig. 3. Complementary filter.

shows a block diagram of the filter. H_{Acc} and H_{Gyro} denote the sensor transfer functions, and G_{Acc} and G_{Gyro} comprise the respective filter function of the sensor. The filter functions are chosen to match the properties of the respective sensor. As proposed in [1], the velocity signal from the gyroscopes is integrated and high-pass filtered. This has the advantage that constant drift is compensated. On the other hand, the orientation computed by the acceleration sensors is low-pass filtered. The time constants of the low- and high-pass filters have to be equal and define the estimation behavior.

A low time constant increases the influence of the acceleration sensor on high-frequency signals and, thus, makes the estimate become sensitive to linear accelerations. Choosing a high time constant takes advantage of the dynamic properties of the gyroscopes, but the time-varying bias is not being compensated fast enough and disturbances decay more slowly. To reduce electromagnetic disturbances, all sensors and the microcontroller are integrated in a closed sensor housing.

III. CONTROL

A. Constraints

The main difficulties in the control of dynamically walking robots result from constraints that limit the applicability of conventional control concepts. Two groups of constraints need to be considered. Firstly the workspace of the joints (1), the maximum rotor velocities (2), and the joint torques (3) are limited

$$\boldsymbol{q}_{min} \leq \boldsymbol{q} \leq \boldsymbol{q}_{max} \tag{1}$$

$$\dot{\boldsymbol{q}}_{min} \leq \dot{\boldsymbol{q}} \leq \dot{\boldsymbol{q}}_{max} \tag{2}$$

$$\boldsymbol{\lambda}_{min}(\dot{\boldsymbol{q}}, \boldsymbol{T}) \leq \boldsymbol{\lambda} \leq \boldsymbol{\lambda}_{max}(\dot{\boldsymbol{q}}, \boldsymbol{T}). \tag{3}$$

These are typical constraints for industrial robots and can be satisfied by an adequate design and an appropriate choice of the trajectories. However, critical control problems result from the second group of constraints that describe the unilateral contact between the feet and the ground. Depending on the normal force $F_{i,z}$, that is, transmit from foot $i = 1, 2$ to the ground, the maximum transmissible torques $T_{i,x}$, $T_{i,y}$, and $T_{i,z}$, as well as the tangential forces $F_{i,x}$ and $F_{i,y}$ are limited by the size of the feet l_x, l_y and the coefficients of friction μ_t, μ_d

$$|T_x| \leq 0.5\, F_z l_y, \qquad |T_y| \leq 0.5\, F_z l_x \tag{4}$$

$$\sqrt{F_x^2 + F_y^2} \leq \mu_t F_z, \qquad F_z \geq 0 \quad |T_z| \leq \mu_d\, F_z. \tag{5}$$

While practical experiments show that the robot usually does not start slipping, the limits of the torques in the lateral and

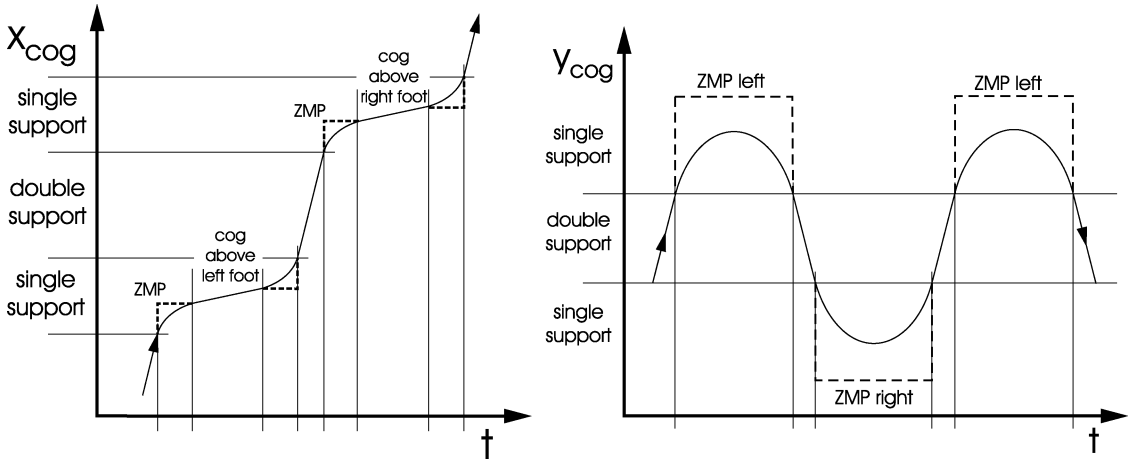

Fig. 4. COG frontal/lateral.

frontal direction T_x and T_y lead to a small margin of stability. Much research has been spent on concepts to ensure that these constraints are satisfied throughout the entire gait cycle. The "Zero Moment Point" (ZMP) theory is one of the most popular approaches to describe the constraints [16].

B. Trajectory Generation

The trajectories of the robot are defined in terms of Cartesian coordinates. These are the position of the center of gravity $\boldsymbol{x}_{\mathrm{cog}}$, the rotation of the upper body $\boldsymbol{\varphi}_U$ and the position and orientation of the foot that is swinging forward $\boldsymbol{x}_{Fs}, \boldsymbol{\varphi}_{Fs}$. Add to this the pelvis joint q_p and the joints of the arms $\boldsymbol{q}_a$ are controlled. Then, $\boldsymbol{x}_{ref} = (\boldsymbol{x}_{\mathrm{cog}}^T\ \boldsymbol{\varphi}_U^T\ \boldsymbol{x}_{Fs}^T\ \boldsymbol{\varphi}_{Fs}^T\ q_p\ \boldsymbol{q}_a^T)^T$ is the vector of controlled variables. Except for the horizontal motion of the center of gravity, the motion of these variables is defined in fifth-order polynomials for each phase of the gait pattern.

The reference trajectories of the center of gravity are computed with a lumped-mass model. These approximations are not completely exact, as the acceleration of the swinging foot does also influence the dynamics of the center of gravity. However, practical experiments have shown that the model is sufficient for walking speeds up to 2.4 km/h.

In the reduced model, it is assumed that the mass of the robot can be lumped to the center of gravity. The motion of the center of gravity in the frontal direction is independent of the motion in the lateral direction. When the center of gravity is kept on a constant height, we obtain a particularly simple solution for the dynamics of the center of gravity. For the lateral direction y_{cog} the acceleration $\ddot{y}_{\mathrm{cog}}$ results in

$$\ddot{y}_{\mathrm{cog}} = \frac{g_z}{z_{\mathrm{cog}}}(y_{\mathrm{cog}} - y_{\mathrm{zmp}}). \tag{6}$$

Here, g_z is the vertical component of the gravity vector, z_{cog} is the height of the center of gravity, and y_{zmp} is the position of the ZMP. During walking, the center of gravity is shifted periodically from one leg to the other such that the legs can alternately swing forward. During the single support phase the lateral position of the zero moment point shall be constant with respect to the supporting foot. For maximum stability margins it can be selected to be in the middle of the foot area, for minimum lateral deviation of the center of gravity it has to be on the inner edge of the supporting foot. The resulting equations for single support are

$$y_{\mathrm{cog}} = c_1 cosh\,(a(t - t_0)) + c_2 sinh\,(a(t - t_0)) \tag{7}$$

with $a = \sqrt{g_z/z_{\mathrm{cog}}}$. The coefficients c_1 and c_2 are computed such that $y_{\mathrm{cog}}(t_0) = y_{\mathrm{cog}}(t_1)$ and $\dot{y}_{\mathrm{cog}}(t_0) = -\dot{y}_{\mathrm{cog}}(t_1)$ with t_0 and t_1 being the beginning and the end of the single support phase. During double support the velocity of the center of gravity shall be constant. The resulting motion of the center of gravity is depicted in the right side of Fig. 4. The velocity of the center of gravity in walking direction is computed according to the same principle. During the single support phase the zero moment point moves from the rear edge of the supporting foot to the front edge. This way the velocity of the center of gravity can be kept constant while it is above the supporting foot. The corresponding motion of the center of gravity in the frontal direction is depicted in the left side of Fig. 4. The simplified model has the advantage that the trajectories can be computed online and, therefore, it is possible to compensate model inaccuracies as well as external disturbances by an adaptation of the trajectories.

C. Computed Torque Method

The computed torque method allows one to consider the entire system dynamics in the control of the robot. The dynamics of the system are denoted as

$$\boldsymbol{M}\ddot{\boldsymbol{q}} + \boldsymbol{W}_1 \begin{pmatrix} \boldsymbol{\lambda}_m \\ T_x \\ T_y \end{pmatrix} = \boldsymbol{h} + \boldsymbol{W}_F \boldsymbol{\lambda}_{FR}. \tag{8}$$

Here, $\boldsymbol{M} \in \mathbb{R}^{21\times 21}$ is the mass matrix of the entire system, $\boldsymbol{q} \in \mathbb{R}^{21}$ are the generalized coordinates and $\boldsymbol{h} \in \mathbb{R}^{21}$ is the vector of nonlinear dynamic terms including the coriolis forces. The forces and torques that act on the system are split up into four terms. T_x and T_y are the lateral and frontal torques between the supporting foot and the ground. These are a function of the torques of the corresponding ankle joint, therefore, the torques

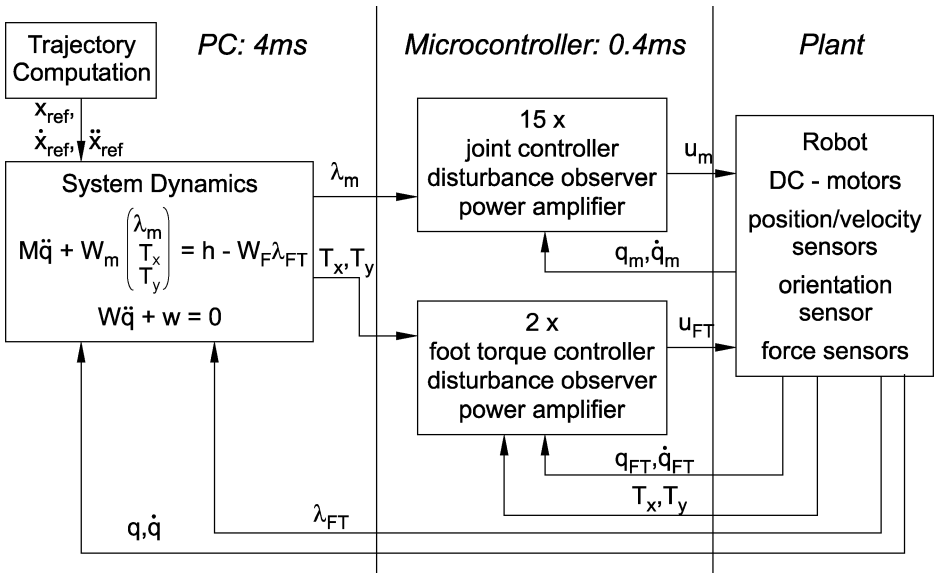

Fig. 5. Computed torque.

of the ankle joint do not explicitly show up in the equations. Vector $\boldsymbol{\lambda}_m$ comprises the remaining 15 joint torques. The forces that act on the supporting foot and the torque around the vertical axis are contained in $\boldsymbol{\lambda}_{FR}$. Using the Jacobians $\boldsymbol{W}_1$ and $\boldsymbol{W}_F$, the torques and forces are mapped on the generalized coordinates.

As described above, the trajectories are computed in terms of Cartesian coordinates $\boldsymbol{x}_{ref} = (x_{\mathrm{cog}}\ y_{\mathrm{cog}}\ z_{\mathrm{cog}}\ \boldsymbol{\varphi}_U^T\ \boldsymbol{x}_{Fs}^T\ \boldsymbol{\varphi}_{Fs}^T\ q_p\ \boldsymbol{q}_a^T)^T \in \mathbb{R}^{17}$. As long as the system is not underactuated, we can define a linear behavior for these variables

$$\ddot{\boldsymbol{x}} = \ddot{\boldsymbol{x}}_{ref} + \boldsymbol{A}_1\Delta\dot{\boldsymbol{x}} + \boldsymbol{A}_2\Delta\boldsymbol{x} + \boldsymbol{A}_3\int\Delta\boldsymbol{x}dt \tag{9}$$

with $\Delta\boldsymbol{x} = (\boldsymbol{x}_{ref} - \boldsymbol{x})$. The Cartesian coordinates are mapped on the generalized coordinates with Jacobian $\boldsymbol{W}_2$, such that

$$\boldsymbol{W}_2\ddot{\boldsymbol{q}} = \ddot{\boldsymbol{x}}_{ref} + \boldsymbol{A}_1\Delta\dot{\boldsymbol{x}} + \boldsymbol{A}_2\Delta\boldsymbol{x} + \boldsymbol{A}_3\int\Delta\boldsymbol{x}dt - \dot{\boldsymbol{J}}\dot{\boldsymbol{q}}. \tag{10}$$

In the following, the control law is summed up in $\boldsymbol{w}$:

$$\boldsymbol{w} = -\left(\ddot{\boldsymbol{x}}_{ref} + \boldsymbol{A}_1\Delta\dot{\boldsymbol{x}} + \boldsymbol{A}_2\Delta\boldsymbol{x} + \boldsymbol{A}_3\int\Delta\boldsymbol{x}dt - \dot{\boldsymbol{J}}\dot{\boldsymbol{q}}\right). \tag{11}$$

The motor torques and the foot torques are computed with (9) and (10) together with the equations of motion (8)

$$\begin{pmatrix}\boldsymbol{\lambda}_m\\ T_x\\ T_y\end{pmatrix} = \begin{array}{c}(\boldsymbol{W}_2\boldsymbol{M}^{-1}\boldsymbol{W}_1)^{-1}\\ \left(\boldsymbol{w} + \boldsymbol{W}_2\boldsymbol{M}^{-1}(\boldsymbol{h} + \boldsymbol{W}_F\boldsymbol{\lambda}_{FR})\right).\end{array} \tag{12}$$

Torque Constraints: The resulting torques lead to the desired system behavior, as long as the limits of T_x and T_y are not exceeded. When the result of (12) violates the constraints from (4), a different set of controlled variables is chosen. For example, when the limits of T_x are exceeded we give up controlling the horizontal position of the center of gravity in the lateral direction y_{cog}. Then the vector of controlled variables has only 16 elements: $\boldsymbol{x}^*_{ref} = (y_{\mathrm{cog}}\, z_{\mathrm{cog}}\, \boldsymbol{\varphi}_U^T\, \boldsymbol{x}_{Fs}^T\, \boldsymbol{\varphi}_{Fs}^T\, q_p\, \boldsymbol{q}_a)^T \in \mathbb{R}^{16}$. Instead of the horizontal position of the center of gravity, we can now

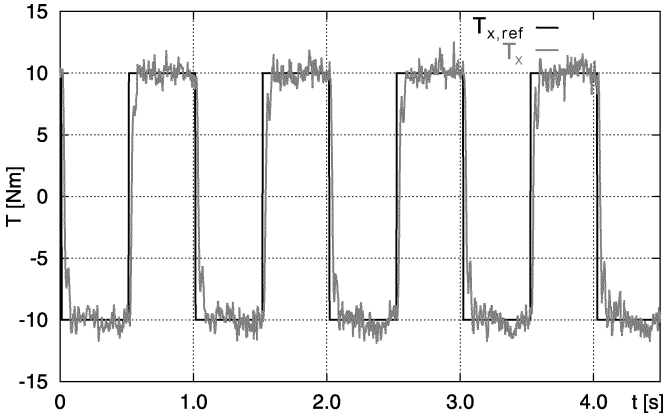

Fig. 6. Torque control.

control the foot torque T_x, which shall be equal to the extreme value ($T_x = T_{x,min}$ or $T_x = T_{x,max}$, respectively). In the resulting equations of motion the limited torque T_x is treated like an external force, which is mapped on the equations of motion with the Jacobian $\boldsymbol{W}_{T,x}$

$$\boldsymbol{M}\ddot{\boldsymbol{q}} + \boldsymbol{W}_1^*\begin{pmatrix}\boldsymbol{\lambda}_m\\ T_y\end{pmatrix} = \boldsymbol{h} + \boldsymbol{W}_F\boldsymbol{\lambda}_{FR} + \boldsymbol{W}_{T,x}T_x. \tag{13}$$

Considering that the mapping of the controlled variables has to be adapted to the reduced set, we introduce the reduced Jacobian $\boldsymbol{W}_2^*$ and the reduced right-hand side $\boldsymbol{w}^*$. Then, the joint torques and the foot torque T_y are computed

$$\begin{pmatrix}\boldsymbol{\lambda}_m\\ T_y\end{pmatrix} = \begin{array}{c}\left(\boldsymbol{W}_2^*\boldsymbol{M}^{-1}\boldsymbol{W}_1^*\right)^{-1}\\ \left(\boldsymbol{w}^* + \boldsymbol{W}_2^*\boldsymbol{M}^{-1}(\boldsymbol{h} + \boldsymbol{W}_F\boldsymbol{\lambda}_{FR} + \boldsymbol{W}_{T,x}T_x)\right).\end{array} \tag{14}$$

The torque in the frontal direction T_y is treated the same way, when it reaches its maximal/minimal value. In this case we give up controlling the horizontal position of the center of gravity in the frontal direction. In the practical implementation it is not necessary to compute both (12) and (14) and all other possible

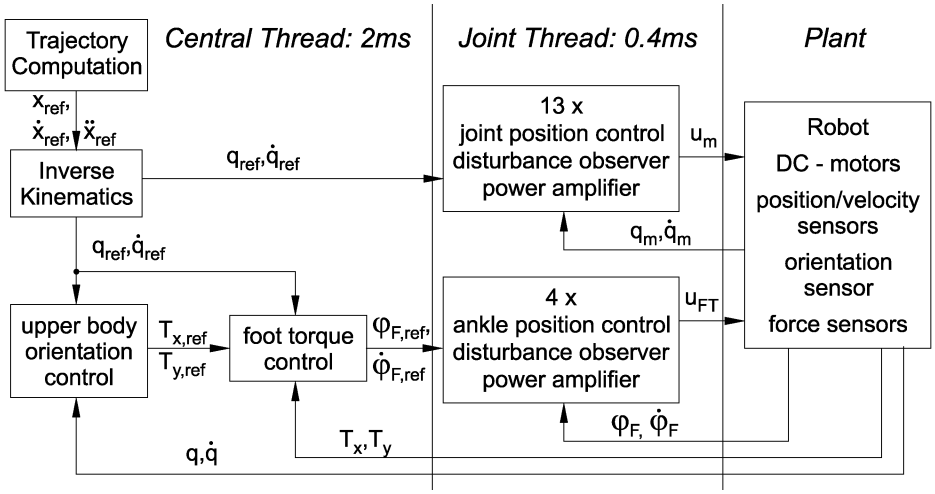

Fig. 7. Trajectory control.

combinations of limited minimal and maximal values of the foot torques. In order to find a valid solution for the torque distribution, it is more efficient to transform the problem into a linear complementarity problem (LCP), which can be solved with less computational effort. Based on the presented scheme, the motor torques are determined consistently for a given limitation of the foot torques. In this way it is ensured that the robot does not tip over in case of disturbances, but it will just accelerate horizontally, which is not critical for the system stability.

The concept to accelerate/decelerate the robot when the upper body tilts forward/backward is known from other papers [5]. However, up to now no consistent solution to determine the system dynamics has been presented for the underactuated case. Using the mapping concept, the exact solution results directly from the set of controlled variables.

The control scheme has been implemented on our biped robot "Johnnie" to realize a dynamically stable walking motion. As shown in Fig. 5, the computation of the reference trajectories and the computation of the system dynamics are performed on a PC running under a real-time LINUX kernel (RTAI). The computed torques are sent to decentral microcontrollers (Infineon C167CS) that drive the power amplifiers and read in the sensor data.

Experiments show that the actual torques of the joints do significantly depend on the time-variant friction of the gears. Therefore, disturbance observers are used to estimate external disturbances as well as varying motor parameters and friction.

As discussed in Section III-A, the foot torques are of particular importance for the system stability. While the actual torques of the joints can only be estimated, it is possible to use the information of the foot torque sensor for the control of the ankle joint.

In our hardware implementation the microcontroller that drives the ankle joint is also used to evaluate the force sensor. This way it is possible to realize a sampling time of 0.4 ms for the torque control of the feet. Experiments have shown that the performance of the torque controller can be improved by a disturbance observer. The performance of the controller is shown in Fig. 6 for a rectangular reference input.

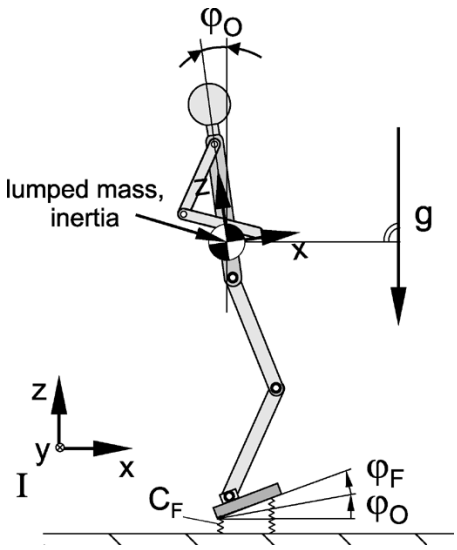

Fig. 8. Inverted pendulum.

D. Problems of the Computed Torque Method

Theoretically, the presented scheme leads to an optimal system performance, since all dynamic effects and the limitation of the foot torques are considered.

The performance of the controller was investigated with the real robot in practical experiments. A walking speed of 1.2 km/h could be achieved with step lengths of 0.35 m. Even though this is in the range of present-state walking machines, it became obvious that the control scheme cannot be used for higher walking speeds. In spite of a fast control of the ZMP, the overall system bandwidth is very low. This is due to three problems.

- Due to the high computational effort, it is not possible to compute the overall system dynamics in less than 4 ms on a Pentium III processor 800 MHz.
- The communication between microcontrollers and PC requires more than 1 ms with the employed CAN-Bus system.
- The orientation sensor has a crossover frequency of 85 Hz, leading to a considerable time delay of the orientation velocity signal.

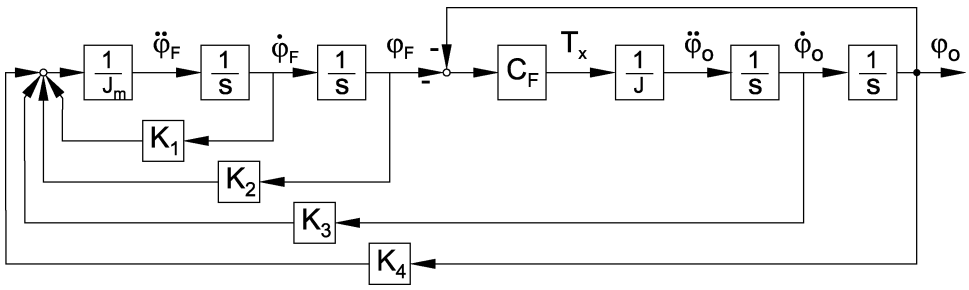

Fig. 9. Control of inverted pendulum model.

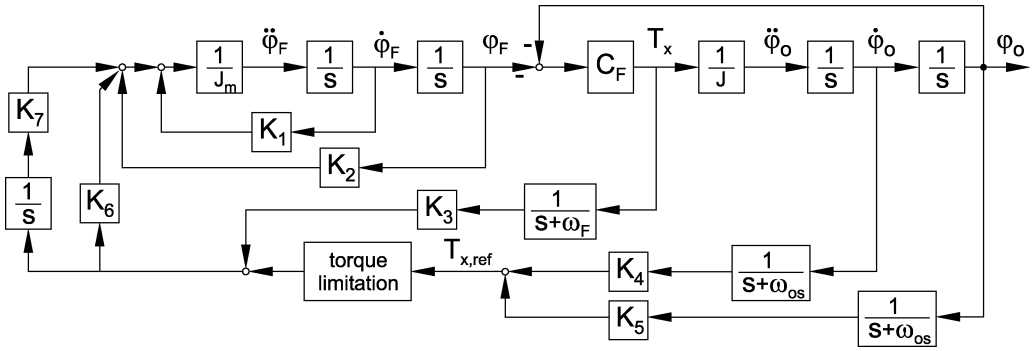

Fig. 10. Control with torque limitation.

The time delay due to the computation time of the PC can be reduced with more efficient algorithms and faster processors, and the communication time can be reduced with a bus system with higher bandwidth. However, it is not possible to obtain an orientation sensor with a significantly higher crossover frequency. Therefore, it cannot be expected that significantly faster gait patterns can be realized with this control scheme.

E. Impedance Control

In order to reach higher walking velocities, a different control approach was investigated that is based on an online adaptation of the trajectories to control the overall posture of the robot. The control scheme is structured in three layers according to Fig. 7. On the highest level is the computation of the reference trajectories as described above. On the second level the trajectories are adapted dependent on the orientation of the robot and the forces that act on the feet. The second level also includes the mapping of the trajectories from Cartesian space to joint space. The lowest level consists of the joint controllers that control the position and velocity of each degree of freedom.

Similar concepts are used to control most of the existing biped robots that can perform a stable walking motion. However, it has not been shown before how to model the system in order to compute the feedback gains to prove stability. The implementations differ in terms of the variables that are used to adapt the trajectories. In most cases the orientation of the supporting foot, i.e., the ankle joint is used to control the foot torques in order to stabilize the robot. Add to this that it is possible to accelerate the upper body horizontally to keep an upright posture. A very popular approach is to also vary the step length in sagittal and lateral direction. Variations of these two parameters have a strong effect on the motion of the robot, however, the implementation is limited by the workspace of the joints. In order to reduce impact when the swinging foot hits the ground, it is possible to introduce some impedance in the vertical position of the feet, i.e., vary the vertical position of the feet with respect to the upper body.

In our robot we have investigated all approaches experimentally, but in the following only the control of the ankle joints will be discussed since it is the most important control parameter.

The dynamics of the robot are linearized around the motion on the reference trajectories. This is possible since the deviations from the reference are assumed to be small. In particular, the inclination of the foot plates differs from the reference position by small angles $\boldsymbol{\varphi}_F = (\varphi_{Fx} \;\; \varphi_{Fy})^T$, while the remaining degrees of freedom of the robot are moving according to the reference trajectories. For a given state of the system, the mass and inertia of the robot are summed together such that we obtain an inverted pendulum model according to Fig. 8.

For a real robot, the contact to the ground always has some compliance. It results from the stiffness of the links, the elasticity of the foot elements, and the compliance of the ground surface. In the model all of these elasticities are combined to a contact stiffness $\boldsymbol{C}_F$. Typically, the damping of the contact is relatively low, and it increases the robustness of the controller. We can, therefore, neglect the damping without loosing the applicability of our approach.

The torques that are transmit from the foot to the ground are

$$\boldsymbol{T}_F = -\boldsymbol{C}_F(\boldsymbol{\varphi}_O + \boldsymbol{\varphi}_F). \tag{15}$$

Here, the angles $\boldsymbol{\varphi}_O$ and $\boldsymbol{\varphi}_F$ denote only the differences of the orientation of the upper body and the foot from the reference trajectory. Also, the torque $\boldsymbol{T}_F$ is the part of the foot torques that results from deviations from the reference trajectory.

Without moving the ankle joints, the dynamics of the system are denoted as

$$\boldsymbol{J}\ddot{\boldsymbol{\varphi}}_O + \boldsymbol{C}_F(\boldsymbol{\varphi}_O + \boldsymbol{\varphi}_F) = 0. \tag{16}$$

When the motion of the joints is independent of the orientation of the upper body $(\boldsymbol{\varphi}_F = \mathbf{0})$, the system is obviously marginally stable. Please note that even without additional control there is a feedback of the position $\boldsymbol{\varphi}_O$ resulting from the compliance of the ground contact. In order to obtain an asymptotically stable system, we have to introduce damping to the system.

For the linearized system, sagittal and lateral dynamics are decoupled, and for each direction we obtain the state equations

$$\begin{pmatrix} \ddot{\varphi}_O \\ \dot{\varphi}_O \\ \ddot{\varphi}_F \\ \dot{\varphi}_F \end{pmatrix} = \begin{pmatrix} 0 & -\frac{C_F}{J} & 0 & -\frac{C_F}{J} \\ 1 & 0 & 0 & 0 \\ 0 & 0 & 0 & 0 \\ 0 & 0 & 1 & 0 \end{pmatrix} \begin{pmatrix} \dot{\varphi}_O \\ \varphi_O \\ \dot{\varphi}_F \\ \varphi_F \end{pmatrix} + \begin{pmatrix} 0 \\ 0 \\ u \\ 0 \end{pmatrix}.$$

The orientation and rotational velocity of the upper body and the position of the foot can be measured such that we can feed back the entire state

$$u = (K_3\ K_4\ K_1\ K_2)(\dot{\varphi}_O\ \varphi_O\ \dot{\varphi}_F\ \varphi_F)^T. \tag{17}$$

A block diagram of the system is depicted in Fig. 9. Obviously, the system is controllable and we can place the poles arbitrarily by choosing $K_1 \ldots K_4$.

In this diagram the limitation of the foot torques due to the length and width of the feet is not considered. It is assumed that the maximum torques are sufficient during normal walking. However, the limits have to be taken into account in case of major disturbances such that the feet do not tilt.

Therefore, a cascaded control structure is used to consider the torque limits according to Fig. 10. The inner loop (feedback K_1 and K_2) consists of a proportional and derivative (PD) control of the joint angles. Here, the transfer function of the motor–gear system and the controller are replaced by a simplified system for conciseness. In the real robot the joint control is augmented with friction observers to obtain a zero steady-state error.

In the outer loop the orientation of the upper body is controlled with the torques of the ankle joint. For this loop the desired torque is computed from the orientation and rotational velocity of the upper body (gains K_4 and K_5). It is limited to the maximum possible value, which depends on the normal force and the size of the feet. The desired value is compared with the measured torque (T_x) and serves as input to the ankle position control (gain K_6). An integral term K_7 allows for compensation of the steady-state error.

In order to get a useful design of the control gains, the transfer functions of the sensors have to be considered. The orientation sensor is approximated by a PT-1 filter, and the force sensors are filtered with a crossover frequency of 250 Hz. Using standard design methods the poles of the closed-loop system can be placed to achieve a high system bandwidth.

Please note that it is not necessary to have a very good tracking of the torque control loop since we are primarily interested in a high robustness of the overall system stability. In fact,

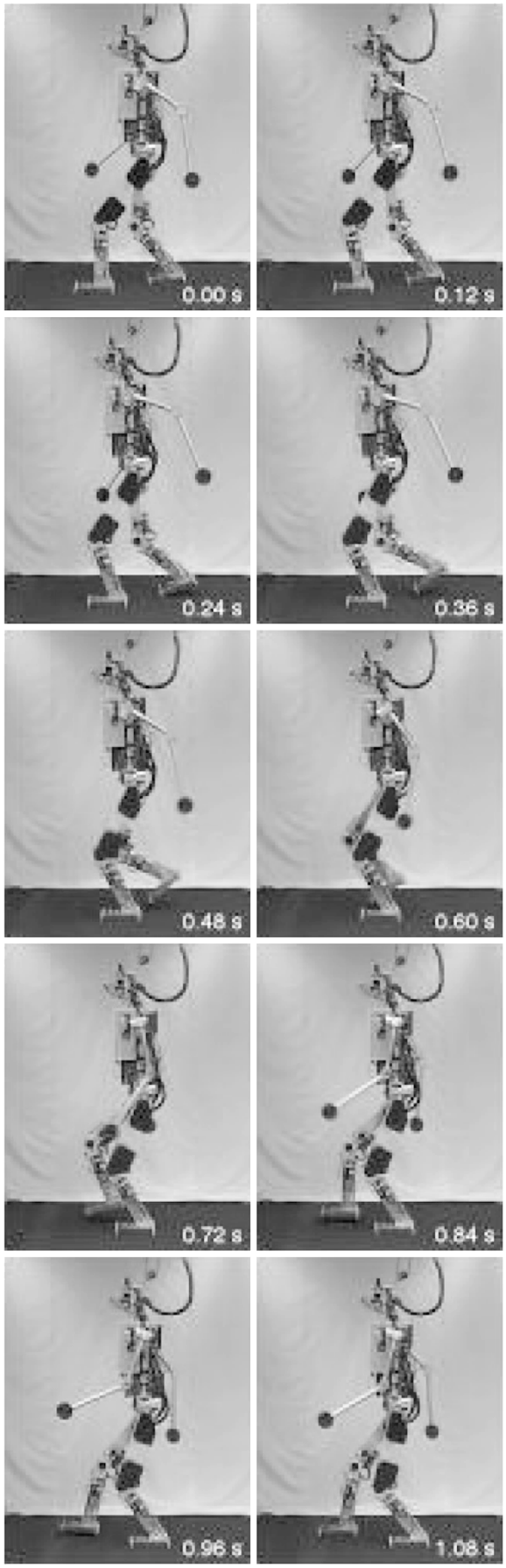

Fig. 11. Johnnie walking.

experiments with a very fast decentralized torque control were not promising. Even though the foot torques could be tracked very quickly, the overall system bandwidth was limited due to a considerable time delay of the orientation sensor. Using the presented approach. instead, the state-space design allows for the choice of a high damping for the overall system.

F. Experiments

The presented control scheme was implemented on a central PC, Pentium IV, 2.8 GHz, and verified in experiments. Presently, stable walking can be realized with up to 2.4 km/h and step lengths of 55 cm. Fig. 11 shows "Johnnie" walking on a conveyor belt.

IV. Conclusion

The sensor system and the control scheme of the humanoid robot "Johnnie" have been presented. In particular, incremental encoders are used to measure the joint angles, while the contact forces to the ground are determined with six-axes force/torque sensors based on strain gauges. A three-axis orientation sensor is used to measure the orientation of the upper body. With the implemented sensor fusion scheme the signal of three gyroscopes and three accelerometers are combined such that the orientation of the upper body can be measured accurately with a crossover frequency of 85 Hz.

Two different control concepts have been investigated. An implementation based on the method of feedback linearization with a decentralized torque control was tested in experiments, but the maximum speed of the robot was limited to 1.2 km/h. In spite of a good control of the foot torques, the overall system bandwidth was not sufficient for higher velocities. Therefore, an impedance control has been implemented that takes into account a simplified model of the overall system. Based on this method a walking speed of 2.4 km/h could be reached in experiments. As the robot has a very lightweight design, it is suitable for fast walking and even for a jogging motion including flight phases. Currently, the corresponding trajectories are being implemented such that higher walking speeds can be realized.

References

[1] A. J. Baerveldt and R. Klang, "A low-cost and low-weight attitude estimation system for an autonomous helicopter," in *Proc. 1997 IEEE Int. Conf. Intelligent Engineering Systems*, Budapest, Hungary, 1997, pp. 391–395.

[2] O. Foellinger, *Regelungstechnik*. Heidelberg, Germany: Hüthig Buch Verlag, 1992.

[3] M. Gienger, K. Löffler, and F. Pfeiffer, "Toward the design of a biped jogging robot," in *Proc. 2001 IEEE Int. Conf. Robotics and Automation*, Seoul, Korea, 2001, pp. 4140–4145.

[4] C. Glocker, *Dynamik von Starrkörpersystemen mit Reibung und Stößen*. Düsseldorf, Germany: VDI-Verlag, 1995.

[5] K. Hirai, M. Hirose, and T. Takenaka, "The development of Honda humanoid robot," in *Proc. 1998 IEEE Int. Conf. Robotics and Automation*, Leuven, Belgium, 1998, pp. 160–165.

[6] J. J. Kuffner, S. Kagami, H. Inoue, M. Inaba, and K. Nishiwaki, "Dynamically stable motion planning for humanoid robots," *Auton. Robots*, vol. 12, pp. 105–118, 2002.

[7] K. Löffler and M. Gienger, "Control of a biped jogging robot," in *Proc. 6th Int. Workshop Advanced Motion Control*, Nagoya, Japan, 2000, pp. 307–323.

[8] K. Löffler, M. Gienger, and F. Pfeiffer, "Sensor and control design of a dynamically stable biped robot," in *Proc. 2003 IEEE Int. Conf. Robotics and Automation*, Taipei, Taiwan, R.O.C., 2003, pp. 484–490.

[9] P. S. Maybeck, *Stochastic Models, Estimation and Control*. New York: Academic, 1979.

[10] F. Pfeiffer, J. Eltze, and H. J. Weidemann, "The TUM-walking machine," *Intell. Automat. Soft Comput.*, vol. 1, pp. 307–323, 1995.

[11] F. Pfeiffer, K. Löffler, and M. Gienger, "The concept of jogging Johnnie," in *Proc. 2002 IEEE Int. Conf. Robotics and Automation*, Washington, DC, 2002, pp. 3129–3135.

[12] S. Riebe and H. Ulbrich, "Modeling and online computation of the dynamics of a parallel kinematic with six degrees-of-freedom," *Arch. Appl. Mech.*, no. 72, pp. 817–829, 2003.

[13] T. Rossmann, *Eine Laufmaschine für Rohre*. Düsseldorf, Germany: VDI-Verlag, 1998.

[14] J. F. Seara, K. H. Strobland, and G. Schmidt, "Path-dependent gaze control for obstacle avoidance in vision guided humanoid walking," in *Proc. 2003 IEEE Int. Conf. Robotics and Automation ICRA*, Taipei, Taiwan, R.O.C., 2003, pp. 887–892.

[15] H. Ulbrich and H. von Stein, *A Combined Feedforward-Feedback Control Strategy for Improving the Dynamics of a Flexible Mechanism*. Norwell, MA: Kluwer, 2002, Multibody System Dynamics, no. 7, pp. 229–248.

[16] J. Vucobratovic, B. Borovac, D. Surla, and D. Stokic, *Biped Locomotion: Dynamics, Stability, Control and Applications*. Berlin, Germany: Springer-Verlag, 1990.

[17] H. J. Weidemann, *Dynamik und Regelung von sechsbeinigen Robotern und natürlichen Hexapoden*. Düsseldorf, Germany: VDI-Verlag, 1993.

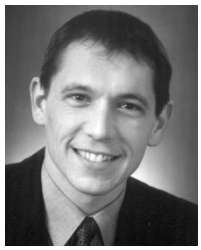

Klaus Löffler was born in Lindau, Germany, in 1972. He received the Master's Degree in mechanical engineering in 1996 from the University of Illinois, Urbana-Champaign, and the Diploma in mechanical engineering in 1998 from the the Technical University of Munich, Garching, Germany, where he is currently working toward the Doctoral degree.

In 1998, he joined the Institute for Applied Mechanics, Technical University of Munich, as a Research Assistant, working on the development of a biped walking robot, in particular, in the area of dynamics and control of the robot. He is currently with BMW AG, Munich, Germany. His areas of interest are research in dynamics and control, robotics, and walking and multibody dynamics.

Michael Gienger was born in Munich, Germany, in 1972. He received the Diploma in mechanical engineering and the Doctoral degree from the Technical University of Munich, Garching, Germany, in 1997 and 2004, respectively.

He wrote his Diploma thesis, "Design of a Strip Cast Edge Trimming Machine," at the University of Vermont. From 1998 to 2003, he was a Research Assistant at the Institute for Applied Mechanics, Technical University of Munich. His project was the "Design and Realization of a Biped Walking Robot." Since 2003, he has been a Researcher at the Honda Research Institute Europe GmbH, Offenbach, Germany. His research interests include the development of walking machines, design, artificial intelligence, and hardware programming.

Friedrich Pfeiffer (M'91–SM'91–F'04) was born in 1935. He received the Diploma and the Doctoral degree in mechanical engineering from the Technische Hochschule Darmstadt, Darmstadt, Germany, in 1961 and 1965, respectively.

From 1966 to 1982, he was with MBB, working in leading positions in the Guided Missile Division. He was also Head of the Theoretical and Technical Mechanics Department at MBB, where, in 1982, he became Vice President R&D of the Guided Missile Division. He was a Full Professor of Mechanics at the Technical University of Munich, Garching, Germany, from 1982 until his retirement in 2000. His areas of interest are research in dynamics and control, nonlinear vibrations, nonlinear machine dynamics, robotics and walking, and transmission systems.

Heinz Ulbrich was born in Hohlen/Sudetenland, Germany, in 1945. He received the Doctoral degree in mechanical engineering from the Technical University of Munich, Garching, Germany, in 1979.

From 1976 to 1981, he was a Research Assistant at the Institute B for Mechanics at the Technical University of Munich, where, from 1981 to 1990, he was Akademischer Oberrat. As a Visiting Researcher, he spent one year (1988–1989) at the NASA Lewis Research Center, Cleveland, OH. From 1990 to 1994, he was Professor of Machine Dynamics and Gear Systems at the TU-Braunschweig, and, from 1994 to 2001, he was a a Full Professor of Mechanics in the Department of Mechanical Engineering, University Essen. Since 2001, he has been Head of the Institute for Applied Mechanics, Department of Mechanical Engineering, Technical University of Munich. His research interests include research in dynamics and control, rotor dynamics, transmission systems, and robotics.